INTERNATIONAL JOURNAL OF ROBUST AND NONLINEAR CONTROL
Int. J. Robust Nonlinear Control 2004; **14**:1035–1059 (DOI: 10.1002/rnc.931)

Robust trajectory tracking for a scale model autonomous helicopter

Robert Mahony[1,*,†] and Tarek Hamel[2]

[1] *Department of Engineering, Australian National University, ACT 0200, Australia*
[2] *I3S, UMR-CNRS 6070, 2000 route des Lucioles, Les algorithmes, Bât Euclide B, 06903 Sophia Antipolis, France*

SUMMARY

This paper considers the question of obtaining an *a priori* bound on the tracking performance, for an arbitrary trajectory, of closed-loop control of an idealized model of a scale model autonomous helicopter. The problem is difficult due to the presence of small body forces that cannot be directly incorporated into the control design. A control Lyapunov function is derived for an approximate model (in which the small body forces are neglected) using backstepping techniques. The Lyapunov function derived is used to analyse the closed-loop performance of the full system. A theorem is proved that provides *a priori* bounds on initial error and the trajectory parameters (linear acceleration and its derivatives) that guarantees acceptable tracking performance of the system. The analysis is expected to be of use in verification of trajectory planning procedures. Copyright © 2004 John Wiley & Sons, Ltd.

KEY WORDS: autonomous helicopters; nonlinear system; Lyapunov control design; robustness analysis

1. INTRODUCTION

There is a growing worldwide interest in the development of scale model autonomous helicopter systems [1, 2]. It appears that the classical modelling and control approaches (cf. for example [3]) are not directly applicable due to the high actuation to inertia ratios and highly nonlinear nature of the rotation dynamics exploited in desired flight conditions for scale model autonomous helicopters. Recently, a number of authors from the control community have begun to investigate an integrated nonlinear dynamic model of a scale model autonomous helicopters (cf. conference papers [4–8] and more recently the journal papers [9–11]). Although the model considered does not contain a sophisticated aerodynamic analysis there is hope that by resolving the basic trajectory planning and control issues for the model considered, it will be possible to extend these developments to provide robust practical controllers for scale model autonomous helicopters. One of the key problems encountered is the presence of significant small body forces leading to weakly non-minimum phase zero dynamics for the full dynamic model. This is a theoretical problem that was also encountered in the investigation of the control of a Vertical Takeoff and Landing Jet (VTOL) [12–16] and [17, p. 246]. Unfortunately, the accepted dynamic

*Correspondence to: Dr. R. Mahony, Department of Engineering, Australian National University, ACT 0200, Australia.
†E-mail: mahony@ieee.org

Received 24 December 2000
Accepted 2 February 2004

model of a helicopter is not feedback linearizable [18–21] and the differential flatness techniques applicable in the case of a VTOL do not apply. Recent work [10] uses trajectory planning to exploit the partial differential flatness properties that do exist for the helicopter model, however, the final stabilizing control design still relies on an approximation of the model. Most other authors have applied a robust control design to the model obtained by ignoring the small body forces and later analyse the performance of the system to ensure that for desired trajectories the un-modelled dynamics do not destroy the stability of the closed-loop system [7, 9, 14]. Such results either take the form of monitoring the behaviour of the system in order to ascertain when the stability guarantees of the control design are broken (cf. Lemma 4.1) or provide some *a priori* guarantees for a restricted class of trajectories [1, 9] (cf. Corollary 4.5). To the authors knowledge no previous work has proposed a robust nonlinear control for a scale model helicopter for which there are *a priori* guaranteed performance bounds given for arbitrary (bounded) trajectories.

In this paper a control design based on backstepping techniques [22] is proposed for a dynamic model of a scale model autonomous helicopter. A control Lyapunov function is derived based on the block pure feedback form [23] of the approximate dynamic model obtained by ignoring the small body forces. The trajectory tracking control design is developed independent of a local co-ordinate parameterization of the helicopter orientation, however, Euler angles are used to parameterize the final 'yaw' parameter that does not explicitly contribute to the flight trajectory dynamics in the idealized model considered. The Lyapunov function obtained for the closed-loop system is used to analyse the performance of the proposed control in tracking an arbitrary trajectory. Firstly, a lemma is given (Lemma 4.1) that monitors the performance of the control relative to the decrease in the Lyapunov function on-line. A much more difficult problem is to provide guaranteed *a priori* bounds of tracking performance for a given trajectory that satisfies certain constraints. Theorem 4.3 provides a result of this nature for arbitrary bounded trajectories. Finally, the particular case of stabilization to a point is considered (the stationary trajectory) and Corollary 4.5 derives a bound on the basin of attraction for the proposed control law applied to this trajectory. The trajectory planning problem is a separate issue of at least equal importance to the control problem considered in this paper. Although the trajectory planning problem is beyond the scope of the present paper the explicit *a priori* bounds on the parameters of a trajectory that may be tracked to within a specified error that are given by Theorem 4.3 are expected to contribute to the design of future trajectory planning algorithms.

The paper is arranged into six sections. Section 2 presents the idealized model of the dynamics of a scale model autonomous helicopter. Section 3 derives a Lyapunov control for an approximate system based on that presented in Section 2 via a backstepping approach. Section 4 contains the main results of the paper and presents the analysis of the closed-loop performance of the proposed control. Section 5 presents a series of experiments which show the behaviour of the closed-loop system for both the approximate and complete dynamic models of the system.

2. DYNAMIC MODEL OF AUTONOMOUS HELICOPTER

In this section, an idealized model for the dynamics of an autonomous scale model helicopter is presented. The model is based on a consideration of the helicopter as a combination of rotor dynamics and rigid body dynamics of the helicopter airframe. Following the lead of

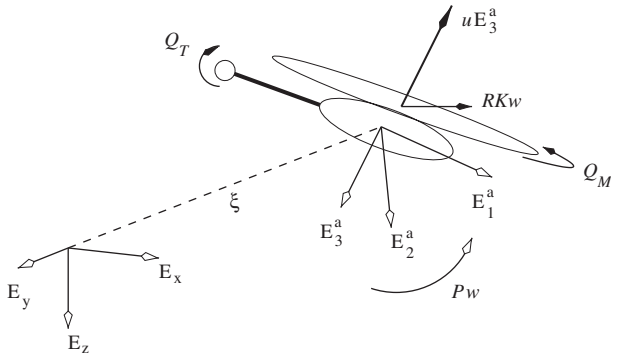

Figure 1. Frames of reference of scale model helicopter and principal forces acting on the airframe.

recent work [5, 7, 9–11] a simple component force model of the rotor dynamics is used. A controller designed for a real world system would need to consider the aerodynamic effects of the rotor dynamics in addition to the nonlinear control problem associated with the airframe dynamics considered in this paper and earlier work. Some work along these lines has been published since the work in this paper was undertaken (cf. References [24, 25] and references therein).

Let $\xi \in \mathbb{R}^3$ denote position of the centre of mass of the helicopter airframe with respect to an inertial frame of reference $\mathscr{I} := \{E_x, E_y, E_z\}$ where E_x etc. denote the co-ordinate axes in the inertial frame. Denote the velocity of the centre of mass as $v = \dot{\xi}$. Let $\mathscr{A} := \{E_1^a, E_2^a, E_3^a\}$ be a body fixed frame attached to the helicopter, where E_1^a is the longitudinal axis of the helicopter frame, E_2^a is the lateral axis and E_3^a is the vertical direction in hover conditions (cf. Figure 1). Let $R : \mathscr{A} \to \mathscr{I}$ be the rotation matrix representing the orientation of $\mathscr{A}$ with respect to $\mathscr{I}$. The angular velocity of $\mathscr{A}$ is represented by a vector $\Omega \in \mathscr{A}$ in the body fixed frame.

In addition to gravitational effect a helicopter is acted on by a number of forces. These forces seen in Equations (2)–(5) are explained in the following list:

$E_3^a u$: The principal rotor provides a strong lift force termed 'heave', oriented along the axis E_3^a in the body fixed frame, which is the principal force responsible to sustaining the helicopter in flight.

$|Q_M|, |Q_T|$: Air resistance on the main and tail rotors result in torques applied directly to the helicopter airframe $|Q_M|$, $|Q_T|$ oriented around the axis of the respective rotor.

Pw: Torque control for the airframe is obtained via a combination of the rigidity of the rotor blades, coriolis forces associated with the effective flapping hinge due to the rotor rigidity, and the induced torques obtained from the deformation of the main rotor disk and consequent tilting of the force vector representing the combined lift generated by the main rotor blades. The vector $w \in \mathbb{R}^3$ represents the contribution to the torque from the deformation of the main rotor disk, the principal mechanism used to obtain control, while the positive definite matrix $P > I_3$ provides the modification for other forces related to rotor rigidity.

$R(\eta)Kw$: Due to the mechanism used to obtain torque control and the consequent tilting of the force vector associated with the main rotor lift, the torque control inputs w are coupled directly to small body forces that affect the translational dynamics of the helicopter airframe. Here K is a constant matrix depending on the physical parameters of the helicopter. It is defined as follows:

$$K = \frac{1}{l_{\mathrm{M}}} \begin{pmatrix} 0 & 1 & 0 \\ -1 & 0 & \frac{1}{l_{\mathrm{T}}} \\ 0 & 0 & 0 \end{pmatrix} \tag{1}$$

where l_{M} and l_{T} denote the offset of the main and tail rotor masts from the centre of mass.

Newton's equations of motion for a helicopter subject to the forces outlined above are

$$\dot{\xi} = v \tag{2}$$

$$m\dot{v} = -E_3^a u + mge_3 + R(\eta)Kw \tag{3}$$

$$\dot{R} = R\mathrm{sk}(\Omega) \tag{4}$$

$$\mathbf{I}\dot{\Omega} = -\Omega \times \mathbf{I}\Omega + |Q_{\mathrm{M}}|e_3 - |Q_{\mathrm{T}}|e_2 + Pw \tag{5}$$

In practice, the model given by Equations (2)–(5) is difficult to control due to the presence of the small body forces which couple torque inputs to translational dynamics (Equation (3)). An approximate model, in which the small body forces are set to zero, is used in the control design

$$\dot{\xi} = v \tag{6}$$

$$m\dot{v} = -E_3^a u + mge_3 \tag{7}$$

$$\dot{R} = R\mathrm{sk}(\Omega) \tag{8}$$

$$\mathbf{I}\dot{\Omega} = -\Omega \times \mathbf{I}\Omega + |Q_{\mathrm{M}}|e_3 - |Q_{\mathrm{T}}|e_2 + Pw \tag{9}$$

The approximate model Equations (2)–(5) is feedback linearizable (and consequently differentially flat). It is a relatively straight forward exercise to obtain a path tracking control algorithm for the approximate model References [4–7, 11]. This model can also be used for trajectory planning problems [10, 11] that exploit the differential flatness properties. However, when a controller designed for the approximate system is applied to the full system dynamics Equations (2)–(5) there is a performance loss. It is the goal of this paper to provide an analysis of the robustness of a controller designed in this manner. We have chosen to use a backstepping control design (in preference to a feedback linearization type design) in order to exploit the natural robustness of such methodology [22] in the robustness analysis undertaken in Section 4.

3. LYAPUNOV BASED TRACKING CONTROL DESIGN

In this section, a backstepping control design is provided for the approximate model (2)–(5) proposed in the previous section.

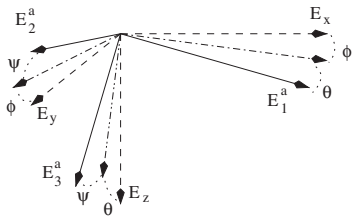

Figure 2. Classical 'yaw-pitch-roll' Euler angles commonly used in aerodynamic applications. Firstly, a rotation of angle ϕ around the axes E_z is applied, corresponding to 'yaw'. Secondly, a rotation of angle θ around the rotated version of the E_y axis is applied, corresponding to 'pitch' of the airframe. Lastly, a rotation of angle ψ around the axes E_1^a is applied. This corresponds to 'roll' of the airframe around the natural axis E_1^a.

Let $\eta = (\phi, \theta, \psi)$ denote the classical 'yaw', 'pitch' and 'roll' Euler angles commonly used in aerodynamic applications [26, p. 608] (cf. Figure 2). The rotation matrix $R := R(\phi, \theta, \psi) \in \mathrm{SO}(3)$ representing the orientation of the airframe **A** relative to a fixed inertial frame may be written[‡] in terms of the Euler angles $\eta = (\phi, \theta, \psi)$

$$R = \begin{pmatrix} c_\theta c_\phi & s_\psi s_\theta c_\phi - c_\psi s_\phi & c_\psi s_\theta c_\phi + s_\psi s_\phi \\ c_\theta s_\phi & s_\psi s_\theta s_\phi + c_\psi c_\phi & c_\psi s_\theta s_\phi - s_\psi c_\phi \\ -s_\theta & s_\psi c_\theta & c_\psi c_\theta \end{pmatrix} \tag{10}$$

The Euler angles $\eta = (\phi, \theta, \psi)$ are not a global co-ordinate patch on SO(3). If $\theta \leqslant \pi/2$ then the correspondence between the Euler co-ordinates and the rotation matrices in SO(3) is one-to-one.

Let

$$\hat{\xi} : \mathbb{R} \to \mathbb{R}^3$$

$$\hat{\phi} : \mathbb{R} \to \mathbb{R}$$

be smooth trajectories $\hat{\xi}(t) := (\hat{x}(t), \hat{y}(t), \hat{z}(t))$ and $\hat{\phi}(t)$. The control objective considered is formally described in the following problem.

Problem
Find a feedback control action (u, w^1, w^2, w^3) depending only on the measurable states $(\dot{\xi}, \xi, \dot{\eta}, \eta)$ and arbitrarily many derivatives of the smooth trajectory $(\hat{\xi}(t), \hat{\phi}(t))$ such that the tracking error

$$\mathscr{E} := (\xi(t) - \hat{\xi}(t), \phi(t) - \hat{\phi}(t)) \in \mathbb{R}^4 \tag{11}$$

converges towards zero for all initial conditions.

[‡]The following shorthand notation for trigonometric function is used.

$$c_\beta := \cos(\beta), \quad s_\beta := \sin(\beta)$$

Define a partial error

$$\delta_1 := \xi(t) - \hat{\xi}(t) \tag{12}$$

comprising that part of the tracking error associated with the position co-ordinates. Define a first storage function

$$S_1 = \tfrac{1}{2}\delta_1^{\mathrm{T}}\delta_1 = \tfrac{1}{2}|\delta_1|^2 \tag{13}$$

Taking the time derivative of S_1 and substituting for Equation (6) yields

$$\begin{aligned}\frac{\mathrm{d}}{\mathrm{d}t}S_1 &= \delta_1^{\mathrm{T}}(\dot{\xi} - \dot{\hat{\xi}}) \\ &= \delta_1^{\mathrm{T}}(v - \hat{v})\end{aligned}$$

where $\hat{v} := \dot{\hat{\xi}}$. Let v_{d} denote a desired value for the velocity v and choose

$$v_{\mathrm{d}} := \hat{v} - \frac{1}{m}\delta_1$$

With this choice one has

$$\begin{aligned}\dot{S}_1 &= \frac{1}{m}\delta_1^{\mathrm{T}}(mv_{\mathrm{d}} - m\hat{v}) + \frac{1}{m}\delta_1^{\mathrm{T}}(mv - mv_{\mathrm{d}}) \\ &= -\frac{1}{m}|\delta_1|^2 + \frac{1}{m}\delta_1^{\mathrm{T}}(mv - mv_{\mathrm{d}})\end{aligned}$$

The process of backstepping continues by considering a new error

$$\delta_2 := mv - mv_{\mathrm{d}}$$

The second storage function considered is

$$S_2 = \tfrac{1}{2}|\delta_2|^2 = \tfrac{1}{2}|mv - mv_{\mathrm{d}}|^2$$

Deriving S_2 and recalling Equation (7) yields

$$\begin{aligned}\dot{S}_2 &= \delta_2^{\mathrm{T}}(m\dot{v} - m\dot{v}_{\mathrm{d}}) \\ &= \delta_2^{\mathrm{T}}(-E_3^a u + mge_3 - m\dot{v}_{\mathrm{d}}) \\ &= \delta_2^{\mathrm{T}}(-uR(\eta)e_3 + mge_3 - m\dot{v}_{\mathrm{d}})\end{aligned}$$

The backstepping process is continued with respect to the new variables (η, u). The control u is explicit in the dynamics of S_2 and could be used directly to partially control the error dynamics. Following this approach leads to a time scale separation of the system dynamics [14, 17]. Such an approach is advantageous in situations such as hover control where the property may be used to ensure that part of the system (e.g. regulating height) is more tightly controlled than other system states. In the case of a VTOL hovering close to the ground this can be a highly desirable characteristic of the control methodology. However, in more general trajectories an artificial time-scale separation imposed in the dynamics at this stage can lead to significant robustness problems. In particular, derivatives of the control u enter into the remaining dynamics of the system and aggressive control may lead to extreme ill-conditioning of the remaining control problem. An alternative strategy is to take a dynamic extension of u

$$\ddot{u} = \tilde{u} \tag{14}$$

The actual control u and its first derivative $\dot{u}$ become internal variables of a dynamic controller. This approach more naturally allows tradeoff between the various control objectives of the generic trajectory tracking problem.

Let (η_d, u_d) denote the desired values of η and the control u and set

$$u_d R(\eta_d) e_3 := mge_3 - m\dot{v}_d + \delta_2 + \frac{1}{m}\delta_1$$

The vectorial value of $u_d R(\eta_d) e_3$ may be arbitrarily assigned for suitable values of η_d and u_d. Note that η_d is not uniquely specified by this relation. The additional freedom in choosing η_d is used later to control the yaw ϕ. It is advantageous to introduce a notation to represent the desired vector input

$$X_d := u_d R(\eta_d) e_3 = mge_3 - m\dot{v}_d + \delta_2 + \frac{1}{m}\delta_1 \tag{15}$$

With the above notation one has

$$\dot{S}_2 = -|\delta_2|^2 - \frac{1}{m}\delta_2^T \delta_1 + \delta_2^T (X_d - uR(\eta)e_3)$$

The process of backstepping continues by considering a third error

$$\delta_3 := u_d R(\eta_d) e_3 - uR(\eta)e_3 = X_d - uR(\eta)e_3 \tag{16}$$

the vectorial difference between the desired and true values of translation thrust $uR(\eta)e_3$ and a further error that penalizes the yaw

$$\varepsilon_3 = \phi - \hat{\phi}$$

The yaw component of the error term is introduced at this stage of the backstepping procedure (rather than along with the initial error term δ_1) in order that the relative degree of δ_3 and ε_3 with respect to the controls $\tilde{u}$ and w match.

Consider the storage function

$$S_3 = \tfrac{1}{2}|\delta_3|^2 + \tfrac{1}{2}|\varepsilon_3|^2$$

Deriving S_3 and recalling Equation (8) yields

$$\dot{S}_3 = \delta_3^T (\dot{X}_d - (\dot{u}R(\eta)e_3 + R(\eta)\mathrm{sk}(\Omega)e_3)) + \varepsilon_3(\dot{\phi} - \dot{\hat{\phi}}) \tag{17}$$

Remark 3.1

The derivative of X_d is computed analytically by differentiating the expression on the right-hand side of Equation (15). The derivatives of u_d and η_d are never explicitly computed.

Consider the term associated with δ_3 firstly. Let $(\Omega_d, \dot{u}_d)$ denote the desired values of Ω and the control derivative $\dot{u}$. Analogously to the case for $uR(\eta)e_3$, the full vectorial term

$$\dot{u}_d R(\eta)e_3 + R(\eta)\mathrm{sk}(\Omega_d)e_3 := \dot{X}_d + \delta_3 + \delta_2 \tag{18}$$

is assigned. Recalling that $\mathrm{sk}(\Omega_\mathrm{d})e_3 = \Omega_\mathrm{d} \times e_3 = -\mathrm{sk}(e_3)\Omega_\mathrm{d}$ Equation (18) may be written as

$$\begin{pmatrix} 0 & 1 & 0 \\ -1 & 0 & 0 \\ 0 & 0 & 1 \end{pmatrix} \begin{pmatrix} \Omega_\mathrm{d}^1 \\ \Omega_\mathrm{d}^2 \\ \dot{u}_\mathrm{d} \end{pmatrix} \coloneqq R(\eta)^\mathrm{T}\left(\dot{X}_\mathrm{d} + \delta_3 + \delta_2\right) \tag{19}$$

It is clear that any vector specified in the right-hand side of Equation (18) may be assigned using only Ω_d^1, Ω_d^2 and $\dot{u}_\mathrm{d}$. This leaves Ω_d^3 free to control the yaw ϕ. Set

$$Y_\mathrm{d} \coloneqq \dot{u}_\mathrm{d} R(\eta)e_3 + R(\eta)\mathrm{sk}(\Omega_\mathrm{d})e_3 = \dot{X}_\mathrm{d} + \delta_3 + \delta_2 \tag{20}$$

Now consider the term associated with ε_3 in Equation (17). The desired input for this term is the yaw velocity of the helicopter $\dot{\phi}$. Let $\dot{\phi}_\mathrm{d}$ denote the desired yaw velocity and choose

$$\dot{\phi}_\mathrm{d} \coloneqq \dot{\bar{\phi}} - \varepsilon_3$$

To proceed it is necessary to recap the kinematic relationship between the Euler angles and the angular velocity of a rigid body. The generalized velocities $\dot{\eta} = (\dot{\phi}, \dot{\theta}, \dot{\psi})$ are related to the angular velocity Ω via standard kinematic relationship [26, p. 609]

$$\dot{\eta} = \frac{1}{\cos(\theta)} \begin{pmatrix} 0 & s_\psi & c_\psi \\ 0 & c_\theta c_\psi & -c_\theta s_\psi \\ c_\theta & s_\theta s_\psi & s_\theta c_\psi \end{pmatrix} \Omega = W_\eta^{-1}\Omega \tag{21}$$

where

$$W_\eta \coloneqq \begin{pmatrix} -s_\theta & 0 & 1 \\ c_\theta s_\psi & c_\psi & 0 \\ c_\theta c_\psi & -s_\psi & 0 \end{pmatrix} \tag{22}$$

Replacing $\dot{\eta}$ by $\dot{\eta}_\mathrm{d}$ and Ω by Ω_d one obtains

$$\dot{\eta}_\mathrm{d} = \frac{1}{\cos(\theta)} \begin{pmatrix} 0 & s_\psi & c_\psi \\ 0 & c_\theta c_\psi & -c_\theta s_\psi \\ c_\theta & s_\theta s_\psi & s_\theta c_\psi \end{pmatrix} \Omega_\mathrm{d}$$

Multiplying by e_1^T one obtains $\dot{\phi}_\mathrm{d} = (s_\psi/c_\theta)\Omega_\mathrm{d}^2 + (c_\psi/c_\theta)\Omega_\mathrm{d}^3$. Assume $\theta, \psi \in (-\pi/2, \pi/2)$ and set

$$\Omega_\mathrm{d}^3 \coloneqq \frac{c_\theta}{c_\psi}\left(\dot{\bar{\phi}} - \varepsilon_3 - \frac{s_\psi}{c_\theta}\Omega_\mathrm{d}^2\right)$$

Thus, the nonlinear coupling of the attitude dynamics leads to a dependence of Ω_d^3 on Ω_d^2 (assigned in Equation (19)).

With the choices made above one may rewrite Equation (17) as

$$\dot{S}_3 = -|\delta_3|^2 - \delta_3^\mathrm{T}\delta_2 - \varepsilon_3^2 + \varepsilon_3(\dot{\phi} - \dot{\phi}_\mathrm{d}) + \delta_3^\mathrm{T}(Y_\mathrm{d} - (\dot{u}R(\eta)e_3 + uR(\eta)\mathrm{sk}(\Omega)e_3)) \tag{23}$$

For the last stage of the backstepping algorithm new error terms are introduced

$$\begin{aligned} \delta_4 &= Y_\mathrm{d} - (\dot{u}R(\eta)e_3 + uR(\eta)\mathrm{sk}(\Omega)e_3) \\ \varepsilon_4 &= \dot{\phi} - \dot{\phi}_\mathrm{d} \end{aligned} \tag{24}$$

With this choice the derivative of S_3 may be written

$$\dot{S}_3 = -|\delta_3|^2 - \delta_3^{\mathrm{T}}\delta_2 - \varepsilon_3^2 + \delta_3^{\mathrm{T}}\delta_4 + \varepsilon_3\varepsilon_4$$

The storage function associated with this stage of the backstepping is

$$S_4 = \tfrac{1}{2}|\delta_4|^2 + \tfrac{1}{2}|\varepsilon_4|^2$$

Thus, taking the derivative of S_4 yields

$$\dot{S}_4 = \delta_4^{\mathrm{T}}(\dot{Y}_{\mathrm{d}} - [\ddot{u}R(\eta)e_3 + 2\dot{u}R(\eta)\mathrm{sk}(\Omega)e_3 + uR(\eta)(\dot{\Omega}\times e_3)]) + \varepsilon_4(\ddot{\phi} - \ddot{\hat{\phi}}) \tag{25}$$

At this stage the control inputs enter into the equations through $\ddot{u} = \tilde{u}, \dot{\Omega}$ via Equation (9) and $\ddot{\phi}$ as seen below.

To simplify the following analysis consider a linearizing control input transformation of Equation (9). Define

$$\tilde{w} := -\mathbf{I}^{-1}\Omega\times\mathbf{I}\Omega + |Q_{\mathrm{M}}|\mathbf{I}^{-1}e_3 - |Q_{\mathrm{T}}|\mathbf{I}^{-1}e_2 + \mathbf{I}^{-1}Pw \tag{26}$$

With this choice Equation (9) becomes $\dot{\Omega} = \tilde{w}$. Taking a second derivative of Equation (21) and regarding only the first component yields

$$\begin{aligned}\ddot{\phi} &= -e_1^{\mathrm{T}}W_\eta^{-1}\dot{W}_\eta W_\eta^{-1}\Omega + e_1^{\mathrm{T}}W_\eta^{-1}\tilde{w}\\ &= -e_1^{\mathrm{T}}W_\eta^{-1}\dot{W}_\eta W_\eta^{-1}\Omega + \frac{s_\psi}{c_\theta}\tilde{w}^2 + \frac{c_\psi}{c_\theta}\tilde{w}^3\end{aligned} \tag{27}$$

Equation (25) may be rewritten as

$$\dot{S}_4 = \delta_4^{\mathrm{T}}(\dot{Y}_{\mathrm{d}} - 2\dot{u}R(\eta)\mathrm{sk}(\Omega)e_3 - [\tilde{u}R(\eta)e_3 - uR(\eta)\mathrm{sk}(e_3)\tilde{w}]) + \varepsilon_4(\ddot{\phi} - \ddot{\hat{\phi}})$$

To achieve the desired control choose

$$\tilde{u}R(\eta)e_3 - uR(\eta)\mathrm{sk}(e_3)\tilde{w} = \dot{Y}_{\mathrm{d}} - 2\dot{u}R(\eta)\mathrm{sk}(\Omega)e_3 + \delta_3 + \delta_4 \tag{28}$$

$$\ddot{\phi} = \ddot{\hat{\phi}} - \varepsilon_4 - \varepsilon_3 \tag{29}$$

With these choices the derivative of S_4 becomes

$$\dot{S}_4 = -|\delta_4|^2 - \delta_4^{\mathrm{T}}\delta_3 - |\varepsilon_4|^2 - \varepsilon_4\varepsilon_3$$

It remains to show that Equations (28) and (29) can be satisfied simultaneously. Rewriting Equation (28) analogously to Equation (19)

$$\begin{pmatrix} 0 & u & 0\\ -u & 0 & 0\\ 0 & 0 & 1\end{pmatrix}\begin{pmatrix}\tilde{w}^1\\ \tilde{w}^2\\ \tilde{u}\end{pmatrix} = R(\eta)^{\mathrm{T}}(\dot{Y}_{\mathrm{d}} - 2\dot{u}R(\eta)\mathrm{sk}(\Omega)e_3 + \delta_3 + \delta_4) \tag{30}$$

As long as $u\neq 0$ the control signals $\tilde{w}^1$, $\tilde{w}^2$ and $\tilde{u}$ are uniquely determined. To obtain $\tilde{w}^3$ one solves for Equation (27) yielding

$$\frac{c_\psi}{c_\theta}\tilde{w}^3 = \ddot{\hat{\phi}} - \varepsilon_4 - \varepsilon_3 + e_1^{\mathrm{T}}W_\eta^{-1}\dot{W}_\eta W_\eta^{-1}\Omega - \frac{s_\psi}{c_\theta}\tilde{w}^2 \tag{31}$$

The above process fully specifies the control inputs $\tilde{w}^1$, $\tilde{w}^2$, $\tilde{w}^3$ and $\tilde{u}$. Using Equations (14) and (26) one recovers the original control inputs u and w, that are themselves functions of more primitive variables of the systems such as flapping angles and thrust components. The

backstepping procedure achieves the monotonic decrease of the Lyapunov function

$$\mathscr{L} \coloneqq S_1 + S_2 + S_3 + S_4$$

This is easily verified by computing

$$\begin{aligned}\dot{\mathscr{L}} &= \dot{S}_1 + \dot{S}_2 + \dot{S}_3 + \dot{S}_4 \\ &= -\frac{1}{m}|\delta_1|^2 - |\delta_2|^2 - |\delta_3|^2 - |\varepsilon_3|^2 - |\delta_4|^2 - |\varepsilon_4|^2 \end{aligned} \tag{32}$$

Recall that δ_1 and ε_3 together form the original tracking error. The error δ_2 regulates the linear velocity of the helicopter. The additional error co-ordinates δ_3 and δ_4 incorporate information on the roll, pitch and their derivatives. This is natural for an under-actuated system since the desired motion can only be obtained by exploiting the attitude dynamics to control the orientation of the thrust. The yaw orientation and its velocity are stabilized independently using the errors ε_1 and ε_2. Applying Lyapunov's second method ensures that $\mathscr{L} \to 0$ along trajectories of the *approximate* system Equations (6)–(9).

4. ANALYSIS

In this section two results are proved that provide bounds on the evolution of the closed-loop system given by Equations (2)–(5) along with the control action given by Equations (30), (31), (14) and (26).

Let

$$\alpha = (\delta_1, \delta_2, \delta_3, \delta_4, \varepsilon_3, \varepsilon_4) \in \mathbb{R}^{14}$$

denote the vector of backstepping errors introduced in Section 3. The error dynamics for the full idealized model Equations (2)–(5) are easily verified to be

$$\dot{\alpha} = \begin{pmatrix} -\frac{1}{m}I_3 & \frac{1}{m}I_3 & 0 & 0 & 0 & 0 \\ -\frac{1}{m}I_3 & -I_3 & I_3 & 0 & 0 & 0 \\ 0 & -I_3 & -I_3 & I_3 & 0 & 0 \\ 0 & 0 & -I_3 & -I_3 & 0 & 0 \\ 0 & 0 & 0 & 0 & -1 & 1 \\ 0 & 0 & 0 & 0 & -1 & -1 \end{pmatrix} \alpha + \begin{pmatrix} 0 \\ R(\eta)Kw \\ \frac{m+1}{m}R(\eta)Kw \\ \frac{2m^2+2m+1}{m^2}R(\eta)Kw \\ 0 \\ 0 \end{pmatrix} \tag{33}$$

The linear block is associated with the feedback linearized structure of the approximate model Equations (6)–(9). The additional perturbations are due to the small body forces in the full idealized model Equations (2)–(5).

In the following analysis, bounds made up of norms of the errors $|\delta_i|,\ i = 1, \ldots, 4$ and $|\varepsilon_3|$ and $|\varepsilon_4|$ are used regularly. To simplify notation define

$$\gamma = (|\delta_1|, |\delta_2|, |\delta_3|, |\delta_4|, |\varepsilon_3|, |\varepsilon_4|) \in \mathbb{R}^6$$

$$\Lambda = \operatorname{diag}\left(\frac{1}{m}, 1, 1, 1, 1, 1\right) \in \mathbb{R}^{6\times 6}$$

$$\chi = (|\dot{\hat{\mathbf{v}}}|, |\hat{\mathbf{v}}^{(2)}|, |\hat{\mathbf{v}}^{(3)}|, |\dot{\hat{\boldsymbol{\phi}}}|, |\hat{\boldsymbol{\phi}}^{(2)}|) \in \mathbb{R}^5$$

Thus, a linear bound in the absolute norms of the error terms may be written $\pi^{\mathrm{T}}\gamma + \tau^{\mathrm{T}}\chi$ for $\pi \in \mathbb{R}^6$, $\tau \in \mathbb{R}^5$, constant vectors. The Lyapunov function $\mathscr{L}$ may be written

$$\mathscr{L} = \tfrac{1}{2}|\gamma|^2 \tag{34}$$

and its time derivative may be written $\dot{\mathscr{L}} = -\gamma^{\mathrm{T}}\Lambda\gamma$ (cf. Equation (32)).

4.1. Online stability analysis

Due to the presence of the small body forces in the error equations (Equation (33)) the Lyapunov function $\mathscr{L}$ may not be monotonically decreasing along solutions of the full model Equations (2)–(5). If the perturbation is small relative to the error α then the linear dynamics in Equation (33) will dominate the perturbations and the Lyapunov function will be decreasing. The following theorem provides an analogous result to that obtained in related works [12, 27].

Lemma 4.1

Consider the dynamics defined by Equations (2)–(5). Let the controls $\tilde{w}$ and $\tilde{\boldsymbol{u}}$ be given by Equations (30) and (31) and recover the control inputs w and $\boldsymbol{u}$ from Equations (14) and (26). Then, the Lyapunov function Equation (34) is strictly decreasing as long as

$$\gamma^{\mathrm{T}}\Lambda\gamma \geqslant \sigma|w|\langle\pi_0, \gamma\rangle \tag{35}$$

where

$$\pi_0 = \left(0, 1, \frac{m+1}{m}, \frac{2m^2+m+1}{m^2}, 0, 0\right) \quad \text{and} \quad \sigma = \frac{1}{l_{\mathrm{M}} l_{\mathrm{T}}}\sqrt{2l_{\mathrm{T}}^2 - 2l_{\mathrm{T}} + 1} = \|K\|_2$$

Proof

Taking the derivative of $\mathscr{L}$, substituting from Equation (33) and using Hölders inequality to bound the effect of the small body forces yields

$$\begin{aligned}\dot{\mathscr{L}} \leqslant & -\gamma^{\mathrm{T}}\Lambda\gamma + |\delta_2|\,|R(\eta)Kw| + \frac{m+1}{m}|\delta_3|\,|R(\eta)Kw| \\ & + \frac{2m^2+m+1}{m}|\delta_4|\,|R(\eta)Kw| \\ = & -\gamma^{\mathrm{T}}\Lambda\gamma + \sigma|w|\pi_0^{\mathrm{T}}\gamma\end{aligned}$$

where π_0 is given in the lemma statement. The result follows directly from this inequality. □

The constant $\sigma = \|K\|_2 \approx \sqrt{2}/l_{\mathrm{M}}$ (for $l_{\mathrm{T}} \gg l_{\mathrm{M}}$) approximately measures the inverse of the offset between the centre of mass of the helicopter and the centre of the rotor disk (at which

point the force u is applied). Thus, σ large corresponds to a small offset and correspondingly large 'small body forces'. The larger the value of σ, the less valid is the approximate model Equations (6)–(9) and the more difficult it is to control the full dynamic model Equations (2)–(5). For a scale model helicopter, a value of $\sigma \approx 2$–5 is typical, corresponding to an offset of around 50–20 cm.

4.2. *Local uniform practical stability analysis*

Lemma 4.1 provides a bound governing the decrease of $\mathscr{L}$ in terms of the size of the small body forces. Such a result is of significant practical importance in proving the asymptotic practical stability of the closed-loop system to a neighbourhood of the desired trajectory. Lemma 4.1, however, does not provide an estimate of the error margin obtained in steady-state tracking. In this section it is shown that the closed-loop system with the full idealized model Equations (2)–(5) is *locally uniformly practically stable* and consequently the error margin for steady-state tracking of a suitable trajectory is bounded.

Definition 4.2
Consider a system with state x. The system is termed *locally uniformly practically stable* around a desired trajectory $\hat{x}$ if there exists constants $k_1, k_2 > 0$ such that for all $|\hat{x}(t)| < k_1$ and initial conditions $|x(0) - \hat{x}(0)| < k_2$ then there exists $k_3 > 0$ such that

$$|x(t) - \hat{x}(t)| < k_3$$

for all time.

Rewrite Equation (26) as follows:

$$Pw = \mathbf{I}\tilde{w} - \Omega \times \mathbf{I}\Omega - |Q_{\mathrm{M}}|e_3 + |Q_{\mathrm{T}}|e_2$$

Since $P(u, w) > I_3$ it follows that $\|P(u, w)\|_2^{-1} \leqslant 1$. Taking the bound on the above equation one obtains

$$|w| \leqslant c_0|\Omega|^2 + c_0|\tilde{w}| + |w_0| \tag{36}$$

where

$$|w_0| = |Q_{\mathrm{M}}| + |Q_{\mathrm{T}}|, \quad c_0 = \|\mathbf{I}\|_2$$

One may think of $|w_0|$ as a bound on the part of the control action w which is necessary to cancel the effect of the anti-torques Q_{M} and Q_{T}.

Due to the nature of the control design it is necessary to consider the torque input $\tilde{w}^3$ separately from the remaining two torque inputs $(\tilde{w}^1, \tilde{w}^2)$. Consider, Equation (31) and note that the singularity associated with the Euler co-ordinates makes it impossible in general to obtain an absolute bound for the value of $|\tilde{w}^3|$. This is a purely mathematical constraint due to the imposition of a particular set of Euler co-ordinates and does not represent a singularity in the physical orientation of the system. By choosing different orientations for the inertial frame $\mathscr{I}$ with respect to which the Euler angles are measured the mathematical singularity may be avoided. Changes of this nature, made at separate finite times, will not alter the remaining control design as long as the trajectory in the new and old representations are related to a smooth trajectory in the general orientation of the helicopter. Assume that the Euler co-ordinates are recomputed relative to a new inertial frame any time one of the angles θ or ψ

exceeds $\pi/4$. Thus, $\cos(\psi), \cos(\theta) > \frac{1}{\sqrt{2}}$. From Equations (22) and (21) the following bounds may be computed:

$$\|W_\eta^{-1}\|_2 \leqslant \frac{1}{\cos\theta} \leqslant \sqrt{2}, \quad \|\dot{W}_\eta\|_2 \leqslant \sqrt{2}|\dot{\eta}|$$

A bound for Equation (31), using these estimates along with the assumed bound on the values of $\cos(\psi)$ and $\cos(\theta)$ is

$$|\tilde{w}^3| \leqslant \langle \tau_1, \chi \rangle + \langle \pi_1, \gamma \rangle + 4|\Omega|^2 + \sqrt{2}|\tilde{w}^2|$$

where

$$\tau_1 = (0, 0, 0, 0, \sqrt{2})^{\mathrm{T}}, \quad \pi_1 = (0, 0, 0, 0, \sqrt{2}, \sqrt{2})^{\mathrm{T}}$$

Let $\tilde{w}^{(1,2)} = (\tilde{w}^1, \tilde{w}^2)$ denote the first two torque inputs for $\tilde{w}$. Thus, multiplying Equation (30) by $\mathrm{sk}(e_3)$ one obtains

$$u\tilde{w}^{(1,2)} = \mathrm{sk}(e_3)R(\eta)^{\mathrm{T}}\dot{Y}_{\mathrm{d}} + 2\dot{u}\,\mathrm{diag}(1, 1, 0)\Omega + \mathrm{sk}(e_3)\delta_3 + \mathrm{sk}(e_3)\delta_4$$

taking norms and bounding this equation one obtains

$$|u||\tilde{w}^{(1,2)}| \leqslant |\dot{Y}_{\mathrm{d}}| + 2|\dot{u}||\Omega| + \langle \pi_2, \gamma \rangle \tag{37}$$

where $\pi_2 = (0, 0, 1, 1, 0, 0)^{\mathrm{T}}$. Now

$$\begin{aligned} |\tilde{w}| &\leqslant |\tilde{w}^{(1,2)}| + |\tilde{w}^3| \\ &\leqslant |\tilde{w}^{(1,2)}| + \langle \tau_1, \chi \rangle + \langle \pi_1, \gamma \rangle + 4|\Omega|^2 + \sqrt{2}|\tilde{w}^2| \\ &\leqslant \frac{(1+\sqrt{2})}{|u|}|u|\,|\tilde{w}^{(1,2)}| + \langle \tau_1, \chi \rangle + \langle \pi_1, \gamma \rangle + 4|\Omega|^2 \end{aligned} \tag{38}$$

Thus, bounding $|u|\,|\tilde{w}^{(1,2)}|$ provides a bound for $|\tilde{w}|$, at least as long as $|u| \neq 0$.

A bound for $|\dot{Y}_{\mathrm{d}}|$ may be obtained via a rather lengthy and uninteresting calculation which involves computing bounds for the various desired signals $|Y_{\mathrm{d}}|$, $|\dot{X}_{\mathrm{d}}|$, $|\dot{v}_{\mathrm{d}}|$ and $|v_{\mathrm{d}}|$ used in the backstepping procedure. One obtains

$$|\dot{Y}_{\mathrm{d}}| \leqslant \langle \tau_2, \chi \rangle + \langle \pi_3, \gamma \rangle + \sigma c_2 |w| \tag{39}$$

where

$$\tau_2 = (0, 0, m, 0, 0)^{\mathrm{T}}, \quad c_2 = \frac{2m^2 + 2m + 1}{m}$$

$$\pi_3 = \left(\frac{2m+1}{m^3}, \frac{2m^3 + m + 1}{m^3}, \frac{2(m+1)}{m}, \frac{2m+1}{m}, 0, 0\right)^{\mathrm{T}}$$

A bound for $|\dot{u}|$ and for $|\Omega|$ can be obtained from Equation (24) along with the bounds obtained for $|Y_{\mathrm{d}}|$. In fact multiplying Equation (24) by $\mathrm{sk}(e_3)$ one obtains a bound for $\Omega^{(1,2)}$ only and not for Ω^3. The bound for Ω^3 is obtained by bounding the first line of Equation (21) and incorporating the expression for $\dot{\phi}_{\mathrm{d}}$ along with the bounds $\cos(\psi), \cos(\theta) > 1/\sqrt{2}$ discussed earlier

$$|\Omega^3| \leqslant |\Omega^2| + \langle \tau_3, \chi \rangle + \langle \pi_4, \gamma \rangle$$

where

$$\tau_3 = (0, 0, 0, \sqrt{2}, 0)^{\mathrm{T}}, \quad \pi_4 = \pi_1$$

Thus, one obtains the following bound for $|\Omega|$:

$$|\Omega| \leqslant 2|\Omega^{(1,2)}| + \langle \tau_3, \chi \rangle + \langle \pi_4, \gamma \rangle$$

Multiplying Equation (24) by e_3^{T} and taking norms one obtains the following bound for $|\dot{u}|$

$$|\dot{u}| \leqslant \langle \tau_4, \chi \rangle + \langle \pi_5, \gamma \rangle \sigma c_3 |w|$$

where

$$\tau_4 = (0, m, 0, 0, 0), \quad c_3 = \frac{m+1}{m^2}$$

$$\pi_5 = \left(\frac{m+1}{m^2}, \frac{1}{m}, \frac{2m+1}{m}, 1, 0, 0 \right)$$

Multiplying Equation (24) by $\mathrm{sk}(e_3)$, taking norms it is seen that $|u||\Omega|$ may be bounded by the same bound used for $|\dot{u}|$. Combining the above results one obtains

$$|\Omega| \leqslant \frac{1}{|u|} (\langle q_1(u), \chi \rangle + \langle p_1(u), \gamma \rangle + \sigma c_4 |w|)$$

where

$$q_1(u) = 2\tau_4 + |u|\tau_3, \quad c_4 = 2c_3, \quad p_1(u) = 2\pi_5 + |u|\pi_4$$

By combining Equations (36), (38) and (39) one obtains

$$|w| \leqslant \frac{1}{|u|} (\langle q_2(u), \chi \rangle + \langle p_2(u), \gamma \rangle + \sigma c_5 |w| + 2|\dot{u}|\,|\Omega| + d_1 |u|\,|\Omega|^2 + |u|\,|w_0|) \tag{40}$$

where $q_2(u) = (1 + \sqrt{2})\tau_2 + |u|\tau_1$, $c_5 = c_2$, $d_1 = 4 + c_0$ and $p_2(u) = (1 + \sqrt{2})\pi_3 + |u|\pi_1 + \pi_2$.

Finally, from Equation (16) one obtains the two sided bound on the control u

$$mg - \langle \tau_5, \chi \rangle - \langle \pi_6, \gamma \rangle \leqslant |u| \leqslant mg + \langle \tau_5, \chi \rangle + \langle \pi_6, \gamma \rangle, \tag{41}$$

where

$$\tau_5 = (m, 0, 0, 0, 0)^{\mathrm{T}}, \quad \pi_6 = \left(\frac{1}{m}, 1, 1, 0, 0, 0 \right)^{\mathrm{T}}$$

The following theorem uses the above development to derive an explicit relationship between a guaranteed bound on the evolution of the Lyapunov function (and hence guaranteed tracking performance) in terms of quantitative bounds on initial conditions, desired trajectories and the physical geometry of the system (in particular the constant σ relating the size of the 'small body forces' to the torque control).

Theorem 4.3

Consider the dynamics defined by Equations (2)–(5). Let the controls $\tilde{w}$ and $\tilde{u}$ be given by Equations (30) and (31) and recover the control inputs w and u using Equations (14) and (26).

Let k_0, k_1 and k_2 be the following initial bounds:

$$|\mathscr{L}(0)| \leqslant k_0^2, \quad |\Omega(0)| \leqslant k_1, \quad |w_0| \leqslant (|Q_{\mathrm{M}}| + |Q_{\mathrm{T}}|) \leqslant k_2$$

Define the auxiliary constants

$$p_3^0 := |mg\pi_1 + \pi_2 + (1+\sqrt{2})\pi_3 + mgd_1k_1\pi_4 + 2k_1(1+d_1)\pi_5|$$

$$p_3^1 := |\pi_1 + d_1k_1\pi_4|$$

$$q_3^0 := |mg\tau_1 + (1+\sqrt{2})\tau_2 + mgd_1k_1\tau_3 + 2k_1(1+d_1)\tau_4|$$

$$q_3^1 := |\tau_1 + d_1k_1\tau_3|$$

$$c_6 := c_5 + 2k_1c_3 + d_1k_1c_4$$

Define two bounding functions for the possible trajectories χ in terms of the available control margin $(mg-\Delta) \leqslant u \leqslant (mg+\Delta)$

$$B_1(\Delta) := \frac{k_0[(mg-\Delta)(1-(\sigma k_2/k_0)|\pi_0|) + \Delta\sigma p_3^1|\pi_0| - \sigma(c_6 + p_3^0|\pi_0|)]}{\sigma(p_3^0 - \Delta p_3^1)(q_3^0 - \Delta q_3^0)} \tag{42}$$

$$B_2(\Delta) := \frac{\Delta - |\pi_6|k_0}{|\tau_5|} \tag{43}$$

Let

$$\Delta_* := \arg \sup_{\Delta \geqslant \left(mg - \frac{k_0(c_4+2|\pi_0|\,|\pi_5|)}{k_1|\pi_0|}\right)} \min\{B_1(\Delta), B_2(\Delta)\}$$

$$B_* := \sup_{\Delta \geqslant \left(mg - \frac{k_0(c_4+2|\pi_0|\,|\pi_5|)}{k_1|\pi_0|}\right)} \min\{B_1(\Delta), B_2(\Delta)\}$$

Then, for any trajectory χ such that

$$|\chi| \leqslant B_*$$

the closed-loop system is uniformly practically stable (cf. Definition 4.2). More precisely,

$$|\mathscr{L}(t)| < k_0^2, \quad \Omega(t) < k_1 + k_0|\pi_0||\pi_4|(mg+\Delta_*) + |\pi_0||q_1(u)|B_*, \quad \textit{and} \quad u > mg - \Delta_* \tag{44}$$

for all time $t \geqslant 0$.

Remark 4.4

(i) Without any further conditions on k_1 and σ there is no *a priori* guarantee that the bounds B_1 and B_2 are positive and the theorem may be null. In practice, the physical constraints of helicopter construction ensure that the bounds are reasonable and lead to practical bounds on possible trajectory choice. Figure 3 shows a plot of $B_1(\Delta)$ and $B_2(\Delta)$ for the helicopter example considered in Section 5.

(ii) Maintaining a lower bound for $|u|$ corresponds to maintaining a positive lift on the main rotor disk at all times.

(iii) A separate bound on the angular velocity Ω is necessary due to the linearization procedure Equation (26). This linearization procedure enters into the analysis via the small body forces and is one of the main sources of complexity in the derivation. The bound K_Ω

(Condition (i)) is slightly larger than the initial condition bound k_1 since an aggressive trajectory choice may result in larger angular velocities than the initial conditions. In practice the angular velocity does not become unbounded for valid trajectories.

Proof

In order to derive the result, the conditions provided by the bounds B_1 and B_2 are transformed into a set of a conditions that are less directly connected to the trajectory planning problem but more closely related to the manner in which the bounds necessary for the proof are derived. Define the following two functions of u:

$$q_3(u) = q_2(u) + 2k_1\tau_4 + d_1k_1q_1(u), \quad p_3(u) = p_2(u) + 2k_1\pi_5 + d_1k_1p_1(u)$$

Due to the bound $B_2(\Delta)$ along with Equation (41) one has

$$mg - \Delta_* \leqslant |u| \leqslant mg + \Delta_*$$

Using this relationship and substituting for previous definitions one obtains the structural form of the constants p_3^0, p_3^1, q_3^0 and q_3^1

$$p_3^0 - \Delta_* p_3^1 \leqslant p_3(u) \leqslant p_3^0 + \Delta_* p_3^1, \quad q_3^0 - \Delta_* q_3^1 \leqslant q_3(u) \leqslant q_3^0 + \Delta_* q_3^1$$

The following three conditions follow from the bounds B_1 and B_2. Condition (i) follows from the limiting condition $\Delta_* \geqslant mg - (k_0(c_4 + 2|\pi_0||\pi_5|)/k_1|\pi_0|)$ in the bounds B_1 and B_2 while Conditions (ii) and (iii) are direct consequences of bounds B_1 and B_2 along with the definitions of $p_3(u)$ and $q_3(u)$:

(i) $|\Omega(0)| < K_\Omega := (1/(mg - \Delta_*)|\pi_0|)(k_0(c_4 + 2|\pi_0||\pi_5|) + k_0|\pi_4|(mg + \Delta_*) + |\pi_0||\tau_5|B_*)$

(ii) $\sigma < (mg - \Delta_*)/(c_6 + |\pi_0||p_3(u)| + (1/k_0)(|p_3(u)||q_3(u)|B_* + (mg - \Delta_*)k_2|\pi_0|))$

(iii) $|\pi_6|k_0 + |\tau_5|B_* < \Delta_*$

It remains to show that these identities lead in turn to the theorem statement.

At time zero, the first bound in Equation (44) is satisfied directly by the theorem statement. The second bound follows from Condition (i). Recall Equation (41) and (at time $t = 0$) apply the bounds $|\mathscr{L}(0)| < k_0^2$ and $\Omega(0) < K_\Omega$. Combining this with Condition (iii) it follows that $u(0) > \Delta_*$. This shows that the bounds are valid at time zero. Moreover, the evolution of the state of the helicopter is smooth and we may proceed using a proof by contradiction.

Assume that the bounds Equation (44) *are not valid for all time*. Then there exist a first time t_0 such that for all $0 \leqslant t < t_0$ the bounds Equation (44) are valid. The contradiction is shown case by case:

Assume that $|u(t_0)| = \Delta_*$ and that $|\mathscr{L}(t)| \leqslant k_0^2$ and $\Omega(t) \leqslant K_\Omega$ on the interval $t \in [0, t_0]$. But now an argument identical to that given in the paragraph above shows that for all $t \in [0, t_0]$ then $|u(t_0)| > mg - \Delta_*$. This ensures that the bound on $|u|$ cannot be the first bound which is broken.

Assume that $|\mathscr{L}(t_0)| = k_0^2$ and that $|u(t)| > mg - \Delta_*$ and $\Omega(t) \leqslant K_\Omega$ on the interval $t \in [0, t_0]$. Using the bound on $\Omega(t) < K_\Omega$ one obtains

$$|\dot{u}||\Omega| \leqslant K_\Omega|\dot{u}|, \quad |\Omega|^2 \leqslant K_\Omega|\Omega|$$

Combining Equations (40) with the parameters given in the theorem statement one obtains the following relation bound on w:

$$|w| \leqslant \frac{1}{mg - \Delta_* - \sigma c_6}(\langle q_3(u), \chi\rangle + \langle p_3(u), \gamma\rangle + (mg - \Delta_*)|w_0|)$$

Observe that Condition (ii) ensures that

$$\sigma < \frac{mg - \Delta_*}{c_6 + |\pi_0||p_3(u)| + a_0}$$

where $a_0 \geqslant 0$. Thus, $mg - \Delta_* - \sigma c_6 > 0$. Substituting into Equation (35) it follows that $\dot{\mathscr{L}}(t) < 0$ if

$$\gamma^{\mathrm{T}} \Lambda \gamma \geqslant \frac{\sigma}{mg - \Delta_* - \sigma c_6} (\gamma^{\mathrm{T}} p_3(u) \pi_0^{\mathrm{T}} \gamma + \gamma^{\mathrm{T}} \pi_0 q_3(u)^{\mathrm{T}} \chi + (mg - \Delta_*)|w_0| \pi_0^{\mathrm{T}} \gamma)$$

But on the interval $t \in [0, t_0]$ one has $\mathscr{L}(t) \leqslant k_0^2$, $|\chi| \leqslant B_*$ and $|w_0| \leqslant k_2$. Applying these bounds in the above equation it may be shown that this condition is equivalent to Condition (ii). Since $\mathscr{L}(0) < k_0^2$ is valid at time zero then $\mathscr{L}(t) < k_0^2$ remains strictly bounded on the interval $t \in [0, t_0]$. This ensures that the bound $\mathscr{L}(t) < k_0^2$ cannot be the first bound which is broken.

Assume that $\Omega(t_0) = K_\Omega$ and that $|u(t)| > mg - \Delta_*$ and $|\mathscr{L}(t)| < k_0^2$ on the interval $t \in [0, t_0]$. Recall that

$$|\Omega| \leqslant \frac{1}{mg - \Delta_*} (\langle q_1(u), \chi \rangle + \langle p_1(u), \gamma \rangle + \sigma c_4 |w|)$$

then substituting for the bound on $|w|$ obtained above one obtains

$$|\Omega| \leqslant \frac{1}{mg - \Delta_*} \left(\langle q_1(u), \chi \rangle + \langle p_1(u), \gamma \rangle + \frac{\sigma c_4}{mg - \Delta_* - \sigma c_6} (\langle q_3(u), \chi \rangle + \langle p_3(u), \gamma \rangle + (mg - \Delta_*)|w_0|) \right)$$

Substituting for the bounds on χ and γ (from the bound on $\mathscr{L}$) it may be shown[§] that the right-hand side is exactly the right-hand side of Condition (i). But then from the conditions of the theorem $|\Omega(t_0)| < K_\Omega$ which contradicts the assumption.

It follows by contradiction that all three bounds are valid for all time. □

An important observation that follows from Theorem 4.3 is the explicit trade off between accuracy of initial condition and the aggressiveness of the goal trajectory. This is best seen by regarding Equation (43) where it is clear that increasing k_0 directly results in a decrease in the bound $B_2(\Delta)$ and is expected to translate into a reduction of the margin B_* available for the trajectory choice. An advantage of the form in which Theorem 4.3 is stated is that the tradeoff between initial condition and tracking performance is naturally incorporated into the analysis and no special cases need to be considered separately.

4.3. Local asymptotic stability for constant trajectories

It is interest to consider the particular case of stabilization to a constant hover position or tracking a desired trajectory with a constant velocity. In this case no margin for the bound B_* need be preserved since $|\chi| \equiv 0$. Assume that the constant rotor drag required for hover is known and pre-compensated such that the remaining air resistance terms Q_{M} and Q_{T} are negligible.

[§] The argument used here is too complicated to include here and adds little insight to the overall proof. Interested readers may obtain the details by contacting the authors.

Corollary 4.5
Consider the dynamics defined by Equations (2)–(5). Let the controls $\tilde{w}$ and $\tilde{u}$ be given by Equations (30) and (31) and recover the control inputs w and u from Equations (14) and (26).

Let k_0 be a bound on the initial condition of the Lyapunov function

$$|\mathscr{L}(0)| \leqslant k_0^2$$

Assume that the anti-torques and the accelerations of the desired trajectories χ are zero

$$|\chi| = 0 \quad \text{and} \quad |Q_{\mathrm{M}}| + |Q_{\mathrm{T}}| = 0$$

If there exists $\Delta > 0$ such that
(i) $|\Omega(0)| < K_\Omega := (1/(mg - \Delta)|\pi_0|)k_0(c_4 + 2|\pi_0||\pi_5| + |\pi_4|(mg + \Delta))$
(ii) $\sigma < (mg - \Delta)/(c_6 + |\pi_0||p_3(u)|)$
(iii) $\Delta > |\pi_6|k_0$

then the control $\tilde{w}$ and $\tilde{u}$, given by Equations (30) and (31) locally asymptotically stabilizes the posture ($\delta_1 \to 0$, $\varepsilon_3 \to 0$) and thus solves stabilization and constant velocity trajectory tracking problems for the complete system Equations (2)–(5).

Proof
Note that the conditions in the Corollary statement are simplified versions of Conditions (i)–(iii) used in the Proof of Theorem 4.3.

The first part of the proof is given by the proof of Theorem 4.3. That is $\mathscr{L}$ is always bounded by k_0^2. Considering that $|u(t)| > \Delta$ and $\Omega(t) < K_\Omega$ for all time and using the bound on $\Omega(t) < K_\Omega$ one obtains

$$|\dot{u}|\,|\Omega| < K_\Omega|\dot{u}|, \quad |\Omega|^2 < K_\Omega|\Omega|$$

Combining Equation (40) with the parameters given in the theorem statement yields the following relation bound on w

$$|w| \leqslant \frac{1}{\Delta - \sigma c_6}\langle p_3(u), \gamma\rangle.$$

Substituting into Equation (35) it follows that $\dot{\mathscr{L}}(t) < 0$ if

$$\gamma^{\mathrm{T}}\left(\Lambda - \frac{\sigma}{\Delta - \sigma c_6}p_3(u)\pi_0^{\mathrm{T}}\right)\gamma \geqslant 0$$

Condition (ii) ensures that

$$\sigma < \frac{\Delta}{c_6 + |\pi_0||p_3(u)|}$$

and consequently the Lyapunov function is strictly decreasing. Classical Lyapunov theory completes the proof. □

5. SIMULATIONS

In this section some simulations indicating the performance of the algorithm proposed in Section 3 are presented.

Theorem 4.3 provides a means of trading off guarantees on tracking performance verses stabilization robustness to initial condition error. In practice, this information is used to provide parameter bounds for trajectory planning algorithms. Note that the bound k_0 on the Lyapunov function measures all the derivatives of the trajectory and not just the position. This is particularly interesting when one considers a trajectory constructed from piecewise smooth template trajectories, such as trimming trajectories [7, 28, 29]. The tradeoff in Theorem 4.3 provides an explicit *a priori* bound on the tracking performance when impulse changes in higher-order derivative terms contributing to the Lyapunov function are introduced.

The following simulations and plots are completed for an example scale model autonomous helicopter with parameters given in Table I. These values represent typical values for scale model autonomous helicopter capable of lifting a payload of around 3–4 kg. The parameters used for the dynamic model are based on preliminary measurements for a VARIO 23cc scale model helicopter owned by HeuDiaSyC (CNRS Laboratory, Université de Technologie de Compiègne).

To provide a perspective on the nature of the bounds and guarantees provided by Theorem 4.3 two plots of the bounding procedure and relationship between k_0 and B_* are provided. A typical example of min sup bound proposed in Theorem 4.3 is shown in Figure 3 for a value of $k_0 = 2$. The values of $k_1 = 0.01$ and $k_2 = 0.002$ were used in the estimates. Note that the min sup of B_1 and B_2 is clearly defined at the intersection of the two graphs. The quadratic nature of the denominator of B_1 leads to a singular asymptote in the plot of B_1 and the intersection of the upper branch with the linear bound B_2 will always lead to the actual value of B_*. As a consequence of this asymptote, the bound on Δ_* never decreases to zero. There is some physical insight in this structure since for the helicopter to achieve any trajectory it is necessary that there is some control margin $mg + \Delta_* > u > mg - \Delta_*$. Since there are always small body forces and initial trajectory errors incorporated in the statement of Theorem 4.3 then a lower bound on Δ_* is expected.

Plotting a figure like Figure 3 for multiple choices of initial condition k_0 it is possible to determine a curve indicating the relationship between k_0 and B_*. This relationship is shown in Figure 4 for the same choices of k_1 and k_2 ($k_1 = 0.01, k_2 = 0.002$).

Consider the case where $k_0 \to 0$ and consequently $\mathscr{L}(0) \to 0$ corresponding to initial conditions that exactly match the desired trajectory motion. In this case the bound B_* converges to a finite limit. This is a physically sensible property since it is clear that for arbitrarily aggressive trajectories the small body forces generated will destroy the tracking properties of the algorithm no matter how small the initial estimate of the Lyapunov function. Effectively, the maximal value of B_* ($B_*^{\max} \approx 0.104$) provides a bound on the guaranteed asymptotic tracking performance of the closed-loop system in the presence of small body forces. In the converse case, as B_* is decreased toward zero, it appears that the initial bound on the Lyapunov function increases to infinity. In practice, there is a physical limit on the control action $0 < mg - \Delta < u$ that limits the range of Δ_*. Applying this constraint in Equation (43) prevents one from using the theoretical min sup measured from Figure 3 and leads to a hard constraint on the maximum initial value of k_0. This physical constraint prevents Corollary 4.5 from being extended to a semi-global asymptotic stability result.

Two simulations of the performance of the closed-loop system have been undertaken. The first experiment considers the case of stabilization of the helicopter dynamics to a stationary configuration given an initial offset. The second considers the case of trajectory tracking. The trajectory chosen for the tracking simulations is a helix ascending in the vertical direction. For

Table I. Parameters of typical scale model autonomous helicopter.

Parameter	Value
Mass	9.6 kg
I_1^a	0.40 kg m^2
I_2^a	0.56 kg m^2
I_3^a	0.29 kg m^2
$\lvert Q_M \rvert$	0.002
$\lvert Q_T \rvert$	0.0002
l_T	1.2 m
l_M	0.27 m
g	9.80 m s^{-2}
σ	3.345

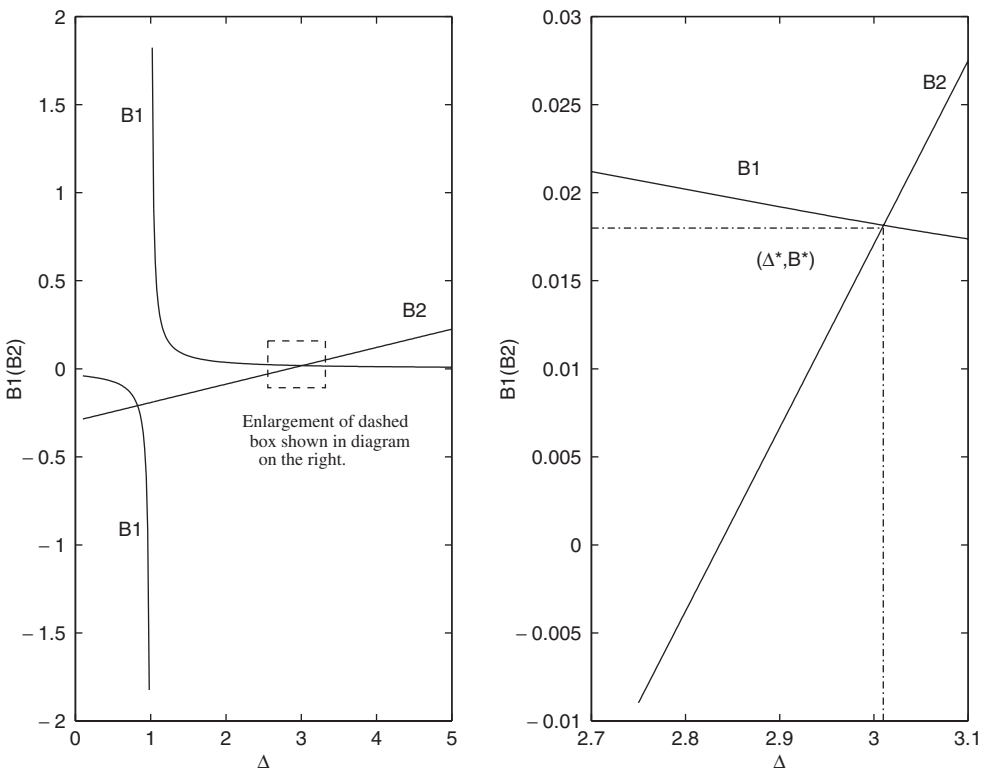

Figure 3. Graph of the bounds B_1 and B_2 with respect to Δ for a fixed value of k_0. The right-hand graph is a close up of the intersection point of the left-hand figure.

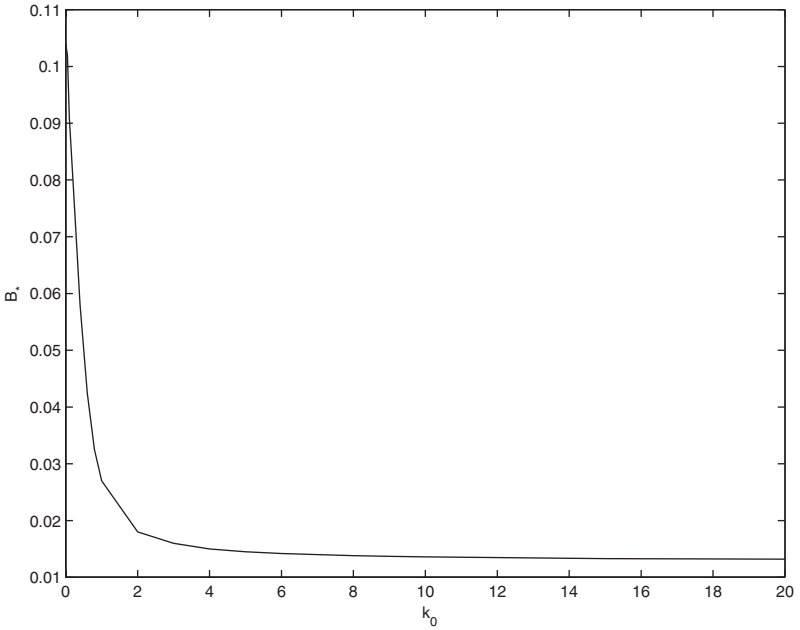

Figure 4. Graph of the relationship between k_0 and B_* for fixed values of k_1 and k_2.

all simulations the helicopter is initially in hover with heave input $u_0 = gm \approx 96$ sustaining its flight. The initial position is

$$\xi_0 = \dot{\xi}_0 = \begin{pmatrix} 0 \\ 0 \\ 0 \end{pmatrix}, \quad \phi_0 = \dot{\phi}_0 = 0$$

In the first simulation the stabilization of position of the helicopter is considered. The desired position $\hat{\xi}_0$ and $\hat{\eta}_0$ are chosen to be

$$\hat{\xi}_0 = \begin{pmatrix} 1 \\ 2 \\ -4 \end{pmatrix}, \quad \hat{\phi}_0 = \frac{\pi}{2}\,\text{rad}$$

The evolution of the dynamic state of a the scale model autonomous helicopter is shown in Figure 5.

The second experiment concerns the problem of tracking a trajectory. In this case, the desired trajectory was chosen as a helix ascending from a point near the centre of mass of the helicopter. The initial condition is characterized by the fact that $\mathscr{L}(0) \approx 7$.

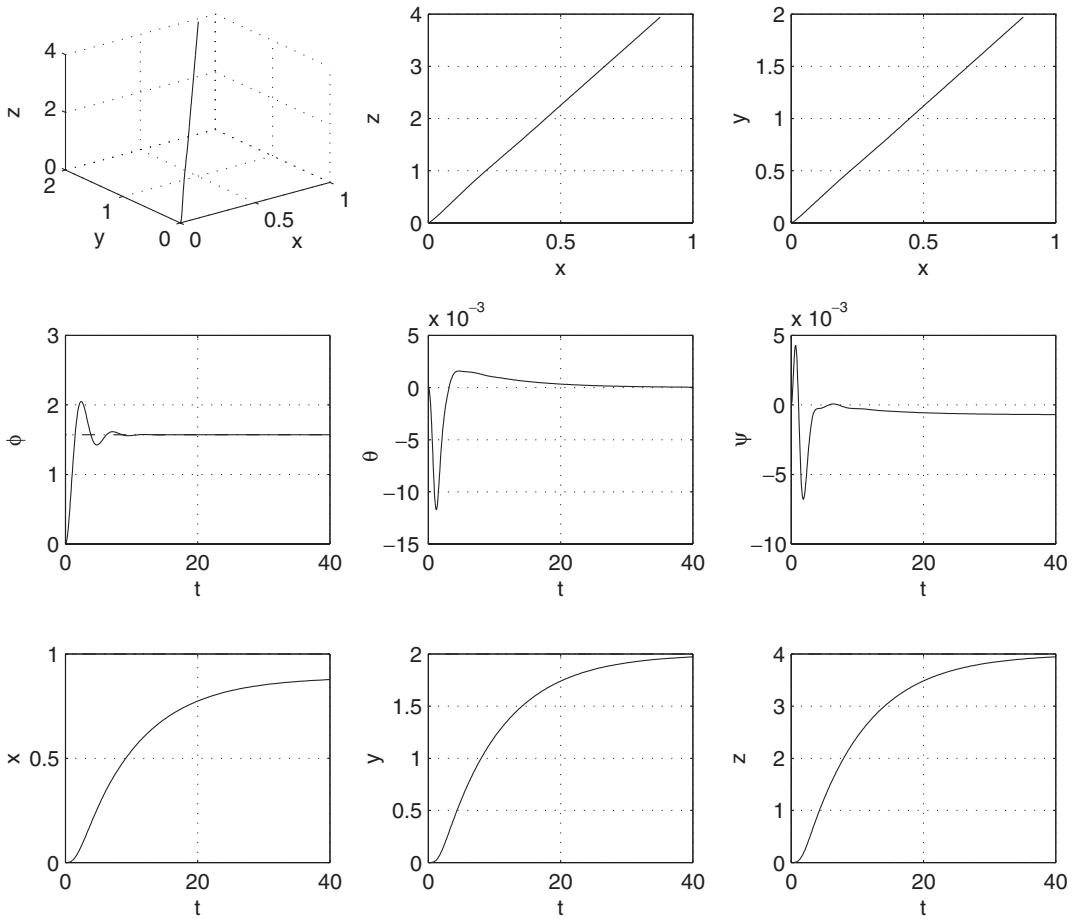

Figure 5. Evolution of the states for the case of stabilization of scale model autonomous helicopter.

The velocity of the desired trajectory is

$$\dot{\xi} = \begin{pmatrix} 0.1\cos\hat{\phi} \\ 0.1\sin\hat{\phi} \\ -0.05 \end{pmatrix}, \quad \dot{\hat{\phi}}_0 = 0.1$$

Thus, $|\chi| \leqslant B_* = 0.0142$. Note that only the derivative (and higher derivatives) of the velocity of the desired trajectory enters into the calculation of χ. Thus, the bound B_* is usually much smaller than a bound directly on derivatives of the velocity of the trajectory. This is important since it allows one to analyse high speed trajectories as long as they are relatively smooth. The evolution of the dynamic state for the second simulation is shown in Figure 6. The evolution of the corresponding Lyapunov function is shown in Figure 7.

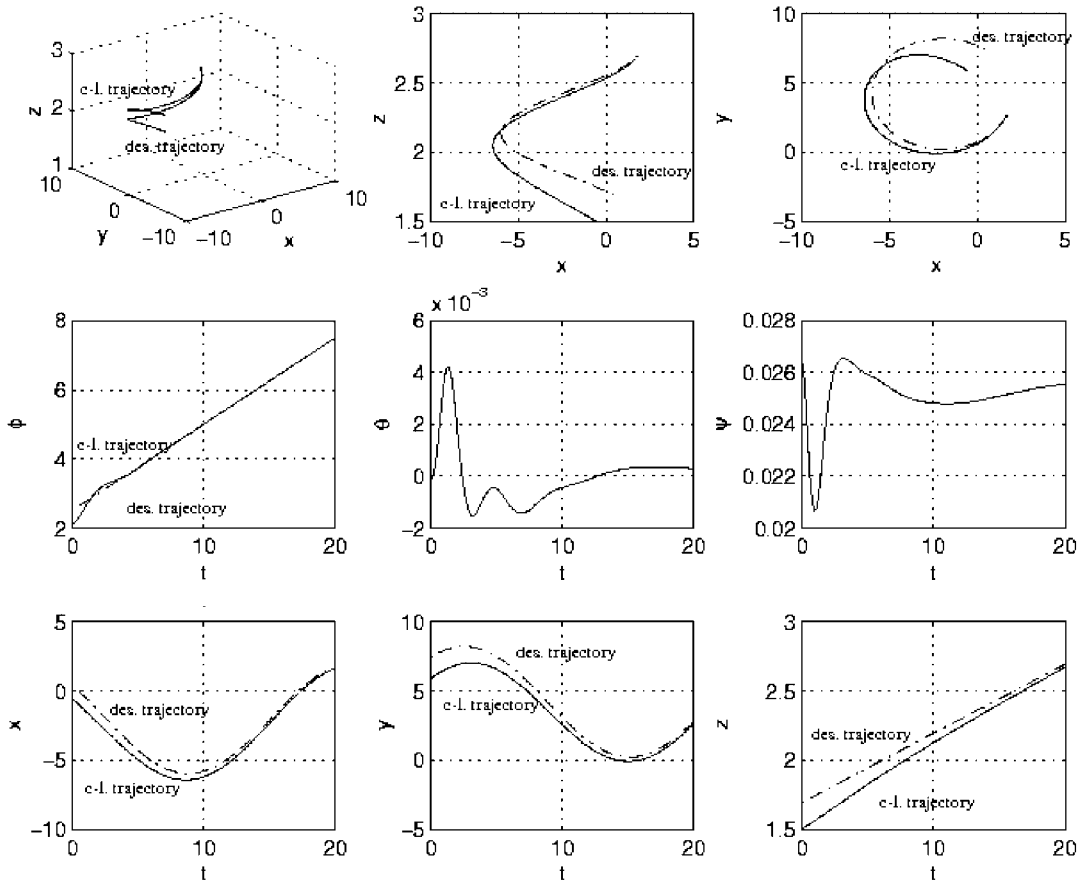

Figure 6. Trajectory tracking for a helicopter in the presence of small body forces. Solid lines show the evolution of the actual trajectory while the dashed lines represent the evolution of the desired one.

6. CONCLUSIONS

In this paper, the question of obtaining an *a priori* bound on the quality of tracking for arbitrary trajectories was considered for a dynamic model of a scale model autonomous helicopter. A Lyapunov control function was derived for an approximate model (in which the small body forces are neglected) using backstepping techniques. Using the robustness of Lyapunov control design approach the dynamics of the closed system was analysed and a theorem was given that provides *a priori* bounds on initial error and the trajectory parameters that guarantee acceptable tracking performance of the system. The analysis is expected to be of use in practical trajectory planning procedures. To the authors knowledge this is the first time that quantitative *a priori* robustness bounds for arbitrary bounded trajectories have been derived for a rigid-body system with 'small body force' dynamic perturbations.

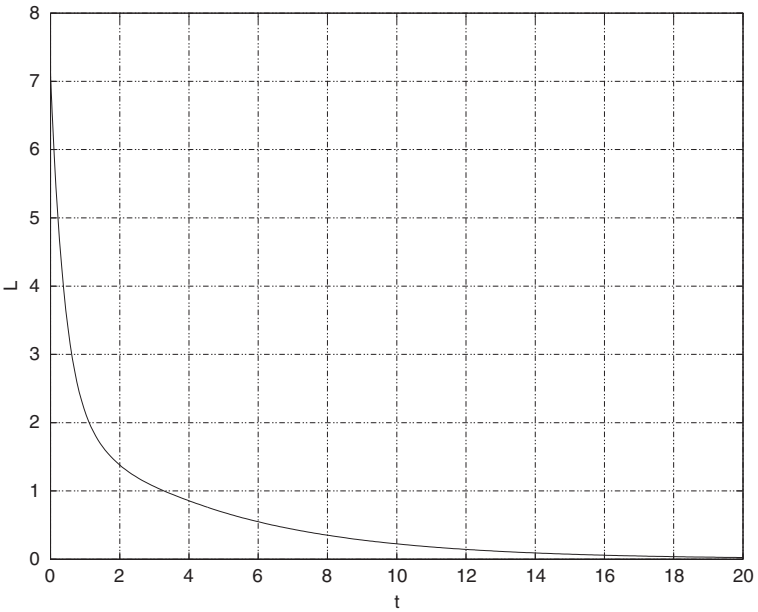

Figure 7. Evolution of the Lyapunov function.

REFERENCES

1. Schaufelberger W, Geering H. *Case Study on Helicopter Control*. Invited session in Control of Complex Systems (COSY) Symposium, Macedonia, October 1998.
2. Koo TJ, Hoffmann F, Shim H, Sastry S. *Control Design and Implementation of Autonomous Helicopter*. Invited session in the Conference on Decision and Control (CDC'98), Florida, 1998.
3. Prouty RW. *Helicopter Performance*, *Stability and Control*. Krieger Publishing Company: New York, 1995 (reprint with additions, original edition 1986).
4. Mahony R, Hamel T, Dzul A. Hover control via approximate Lyapunov control for a model helicopter. In *Proceedings of the 1999 Conference on Decision and Control*, 1999.
5. Sira-Ramirez A, Castro-Linares R, Licéaga-Castro E. Regulation of the longitudinal dynamics of an helicopter system: a Liovillian systems approach. In *Proceedings of the American Control Conference ACC'99*, 1999.
6. Shim H, Koo T, Hoffmann F, Sastry S. A comprehensive study of control design for an autonomous helicopter. In *Proceedings of the 37th Conference on Decision and Control CDC'98*, 1998.
7. Frazzoli E, Dahlen M, Feron E. Trajectory tracking control design for autonomous helicopters using a backstepping algorithm. *Proceedings of the American Control Conference ACC*, 2000; 4102–4107.
8. van Nieuwstadt M, Murray R. Outer flatness: trajectory generation for a model helicopter. In *Proceedings of the European Control Conference* (*CD-ROM*), 1997.
9. Shakernia O, Ma Y, Koo T, Sastry S. Landing an unmanned air vehicle: vision based motion estimation and nonlinear control. *Asian Journal of Control* 1999; **1**(3):128–145.
10. Sira-Ramirez H, Castro-Linares R, Liceaga-Castro E. A Liouvillian systems approach for the trajectory planning-based control of helicopter models. *International Journal of Robust and Nonlinear Control* 2000; **10**:301–320.
11. van Nieuwstadt MJ, Murray RM. Real time trajectory generation for differentially flat systems. *International Journal of Robust and Nonlinear Control* 1997; 1–27.
12. Hauser J, Sastry S, Meyer G. Nonlinear control design for slightly nonminimum phase systems: applications to V/STOL aircraft. *Automatica* 1992; **28**(4): 665–679.
13. Ghanadan R. Nonlinear control system design via dynamic order reduction. *Proceedings of the Conference on Decision and Control*, 3752–3757.
14. Teel AR. A nonlinear small gain theorem for the analysis of control systems with saturation. *IEEE Transactions on Automatic Control* 1996; **41**(9):1256–1270.

15. Martin P, Devasia S, Paden B. A different look at output tracking: control of a VTOL aircraft. *Automatica* 1996; **32**(1):101–107.
16. Murray R, Rathinam M, van Nieuwstadt M. An introduction to differential flatness of mechanical systems. In *Proceedings of Ecole d'Eté, Théorie et practique des systémes plats*, 1996.
17. Sepulchre R, Janković M, Kokotović P. *Constructive Nonlinear Control*. Springer: London, 1997.
18. Thomson D, Bradley R. Recent developments in the calculation of inverse dynamic solutions of the helicopter equations of motion. In *Proceedings of the U.K. Simulation Council Triennial Conference*, 1987.
19. Liceaga-Castro E, Bradley R, Castro-Linares R. Helicopter control design using feedback linearization techniques. *Proceedings of the 28th Conference on Decision and Control*, *CDC'89*, 1989; 533–534.
20. Mallhaupt P, Srinivasan B, Levine J, Bouvin D. A toy more difficult to control than the real thing. *Pages CD-ROM Version of*: *Proceedings of the European Control Conference*, 1997.
21. Mahony R, Lozano R. (Almost) exact path tracking control for an autonomous helicopter in Hover manoeuvres. In *Proceedings of the International Conference on Robotics and Automation*, *ICRA2000*, 2000.
22. Freeman RA, Kokotović PV. Robust nonlinear control design: state-space and Lyapunov techniques. *Systems and Control*: *Foundations and Applications*. Birkhäuser: Boston, U.S.A., 1996.
23. Krstic M, Kanellakopoulos I, Kokotovic PV. *Nonlinear and Adaptive Control Design*. American Mathematical Society: Providence, RI, U.S.A.; 1995.
24. La Civita M. Integrated modeling and robust control for full-envelope flight of robotic helicopters. *Ph.D.*, Department of Mechanical Engineering, Carnegie Mellon University, Pittsburgh, Pennsylvania, 2002.
25. Mettler B. *Identification Modeling and Characteristics of Miniature Rotorcraft*. Kluwer Academic Publishers: The Netherlands, 2003.
26. Goldstein H. *Classical Mechanics* (2nd edn). Addison-Wesley Series in Physics, Addison-Wesley: U.S.A., 1980.
27. Koo TJ, Sastry S. Output tracking control design of a helicopter model based on approximate linearization. In *Proceedings of the IEEE Conference on Decision and Control CDC'98*, 1998.
28. Kaminer I, Pascoal A, Hallberg E, Silvestre C. Trajectory tracking for autonomous vehicles: an integrated approach to guidance and control. *Journal of Guidance and Control* 1998; **21**(1):29–38.
29. Hallberg E, Kaminer I, Pascoal A. Flight test system for unmanned air vehicles. *IEEE Control Systems Magazine* 1999; **19**(1):55–65.

